Iron Oxide Nanorods

DOI: 10.1002/anie.201107113

Rod-Shaped Fe_2O_3 as an Efficient Catalyst for the Selective Reduction of Nitrogen Oxide by Ammonia**

Xiaoling Mou, Bingsen Zhang, Yong Li, Lide Yao, Xuejiao Wei, Dang Sheng Su, and Wenjie Shen**

Selective catalytic reduction (SCR) of nitrogen oxides (NO_x) with NH_3 is nowadays the most promising technology for eliminating nitrogen oxides that are emitted from combustion of fossil fuels.[1] Vanadia-based catalysts are commonly used for this reaction in stationary sources, such as coal-fired power plants and energy use in industry. This mature system displays adequate activity typically at 300–400 °C, but it is still not satisfactory with respect to the volatility and toxicity of VO_x and the easy deactivation.[1–3] Attracted by the inherently environmentally benign character and the prominent thermal stability, ferric oxides have long been explored to catalyze selective reduction of NO_x with ammonia,[3–8] but no significant progress has been achieved so far. Ferric oxides commonly suffer from the insufficient activity at low temperatures and the severe deactivation induced by H_2O and SO_2 that are permanently and abundantly present in the exhaust. On the other hand, studies on crystal phase and shape control of Fe_2O_3 nanomaterials are of great interest in materials science and are actively being pursued in recent years.[9–14] However, most of the synthetic strategies involve high-temperature treatments, yielding undesired mixtures of ferric oxide polymorphs owing to diverse phase transitions.[9] To date, there still remains a challenge to effectively tailor the shape and the crystal phase of Fe_2O_3 materials at nanometer level. Herein, we show that γ-Fe_2O_3 nanorods, which preferentially expose the reactive facets by crystal-phase and morphology control through a solution-based approach, efficiently catalyze selective reduction of NO with NH_3.

We started with shape-controlled synthesis of β-FeOOH nanorods by precipitation of ferric chloride with sodium carbonate in aqueous solution containing poly(ethylene glycol) (PEG) at 120 °C. Scanning electron microscopy (SEM) and transmission electron microscopy (TEM) micrographs show that the obtained β-FeOOH has a rod-like structure with a diameter of 30–50 nm and a length of 350–500 nm (Figure S1 in the Supporting Information). When viewed along the [10$\bar{1}$] (Figure 1a) and [100] directions (Figure 1b) by means of high-resolution TEM (HRTEM), it can be seen that the {010} planes of the nanorod are dominantly exposed. Together with the square-shaped cross section (Supporting Information, Figure S1), the β-FeOOH nanorod is determined to be a rectangular block that is enclosed by two {100} flat planes, two {010} side planes, and two {001} end planes (Figure 1c).

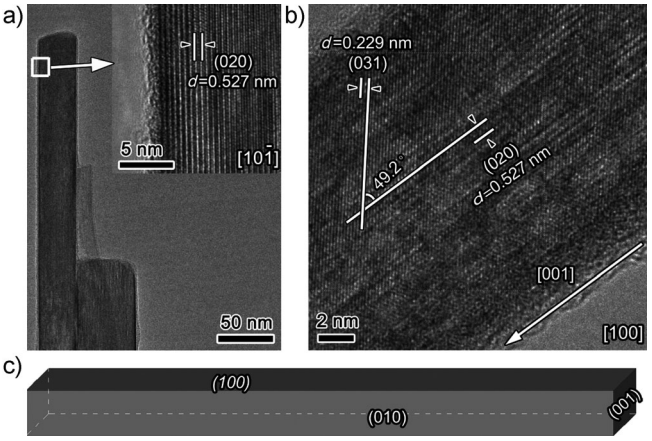

Figure 1. a) A low-magnification TEM image of a single β-FeOOH nanorod viewed along the [10$\bar{1}$] direction.The insert HRTEM image indicates that the nanorod exposes the {010} planes. b) Another HRTEM image viewed along the [100] orientation, also showing the preferential exposure of the {010} planes. c) The real shape of the β-FeOOH nanorod.

γ-Fe_2O_3 nanorods were then obtained by refluxing the β-FeOOH precursor in PEG at 200 °C. An X-ray powder diffraction (XRD) pattern (Supporting Information, Figure S2) shows that the diffraction lines of the (400) and (440) planes are intensified significantly, whereas those of the (422) and (511) planes are weakened considerably compared to the standard powder reflection pattern, which is indicative of anisotropic growth of the {110} and {100} planes. SEM and TEM observations reveal that the γ-Fe_2O_3 nanorods have an average diameter of 40 nm and a mean length of 400 nm (Supporting Information, Figure S3). Moreover, the γ-Fe_2O_3

[*] X. Mou, Dr. Y. Li, X. Wei, Dr. W. Shen
State Key Laboratory of Catalysis, Dalian Institute of Chemical Physics, Chinese Academy of Sciences
Dalian 116023 (China)
E-mail: shen98@dicp.ac.cn
Dr. B. Zhang, Dr. D. S. Su
Shenyang National Laboratory for Materials Science
Institute of Metal Research, Chinese Academy of Sciences
Shenyang 110016 (China)
Dr. L. Yao, Dr. D. S. Su
Department of Inorganic Chemistry
Fritz-Haber Institute of the Max Planck Society
Faradayweg 4–6, 14195 Berlin (Germany)
E-mail: dangsheng@fhi-berlin.mpg.de

[**] We acknowledge the financial support for this research work from the National Nature Science Foundation of China (20923001, 21025312).

Supporting information for this article is available on the WWW under http://dx.doi.org/10.1002/anie.201107113.

nanorods have mesopores of about 22 nm in diameter that have open structures and are isolated from each other, yielding a high surface area of 120 $m^2 g^{-1}$. Iron oxyhydroxide can be easily dehydrated into iron oxide, but the crystal phase varies largely depending on the rearrangement of Fe^{3+} and O^{2-} ions.[15] β-FeOOH has the least dense crystalline structure among its polymorphs and usually dehydrates to α-Fe_2O_3 upon heating.[16] We obtain, as expected, α-Fe_2O_3 nanorods by calcining the β-FeOOH precursor at 500 °C in air (Supporting Information, Figure S4). When heated to reflux in PEG, the β-FeOOH precursor is surprisingly converted into γ-Fe_2O_3 nanorods owing to the moderate water removal manner that benefits the crystallization of maghemite. Ferric oxide has four polymorphs, and the phase transition is strongly dependent on the size of the particles, especially at the nanometer level.[9,17,18] Therefore, we examined the crystal-phase stability of the γ-Fe_2O_3 nanorods by an in situ XRD experiment (Supporting Information, Figure S5). The characteristic (311) and (400) diffraction lines of γ-Fe_2O_3 remain stable up to 600 °C with only slightly weakened intensities. Moreover, the rod shape is also well maintained even if the γ-Fe_2O_3 nanorods were calcined at 550 °C for 5 h in air. All of these results show the exceptionally high crystal-phase and shape stabilities of the γ-Fe_2O_3 nanorods that are a consequence of the unique morphological feature.

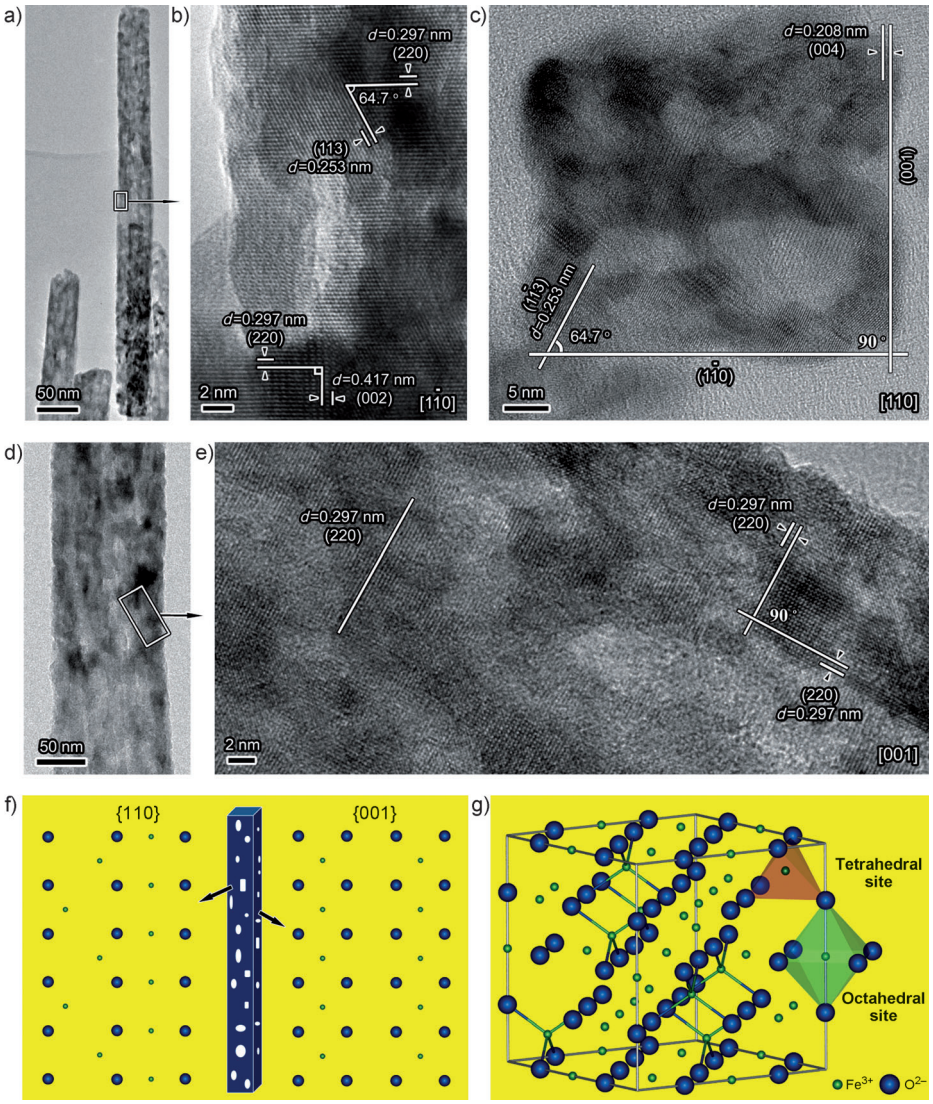

Figure 2. a) Low- and b) high-magnification TEM images of a single γ-Fe_2O_3 nanorod, indicating the dominant exposure of the {110} and {001} planes. c) A square-shaped cross-section of the single rod near the [110] orientation, which is constructed by two side $(1\bar{1}0)$ and (001) planes with a lattice angle of 90°. d) Low- and e) high-magnification TEM images of another γ-Fe_2O_3 nanorod viewed along the [001] direction where the (220) planes are preferentially exposed. f) The real shape of the nanorod and the surface atomic configurations of the preferentially exposed {110} and {001} planes. g) Atomic illustration of a cubic symmetry (space group $Fd\bar{3}m$) and the coordination patterns of tetrahedral and octahedral Fe^{3+} ions.

The crystallographic nature of the γ-Fe_2O_3 nanorods was further examined by HRTEM. Figure 2a shows a single γ-Fe_2O_3 nanorod growing along the $[1\bar{1}0]$ direction. The interplanar distances of 0.253, 0.297, and 0.417 nm on the enlarged image (Figure 2b) correspond to the lattice fringes of the {113}, {110}, and {001} planes, respectively. The square-shaped cross-section viewed near the [110] orientation is constructed by $(1\bar{1}0)$ and (001) as side planes (Figure 2c). When viewed along the [001] direction, the nanorod dominantly exposes the {110} planes (Figure 2d,e). Taking all the analyses into account, the nanorod is constructed with two {110} as end planes, and two {110} and two {001} as side planes (Figure 2f). It is noteworthy that these surfaces are terminated simultaneously by Fe^{3+} and O^{2-} sites.[19–21] There are equal numbers of octahedral and tetrahedral Fe^{3+} ions on the {110} plane (4.05 atoms per nm^2), but only octahedral Fe^{3+} ions on the {001} plane (5.72 atoms per nm^2) (Figure 2g and Supporting Information, Figure S3). Consequently, the surface of the γ-Fe_2O_3 nanorod is relatively rich in octahedral Fe^{3+} ions. More importantly, the length of the Fe–O bond (0.2091 nm) is greater than that in the tetrahedrally coordinated environment (0.1837 nm),[20] making it more reducible and reactive.

Figure 3a shows the catalytic performance of the γ-Fe_2O_3 nanorods in SCR of NO with NH_3. The light-off temperature (the temperature at which the conversion of NO reaches 50%) is as low as 170 °C, and 100% NO conversion is

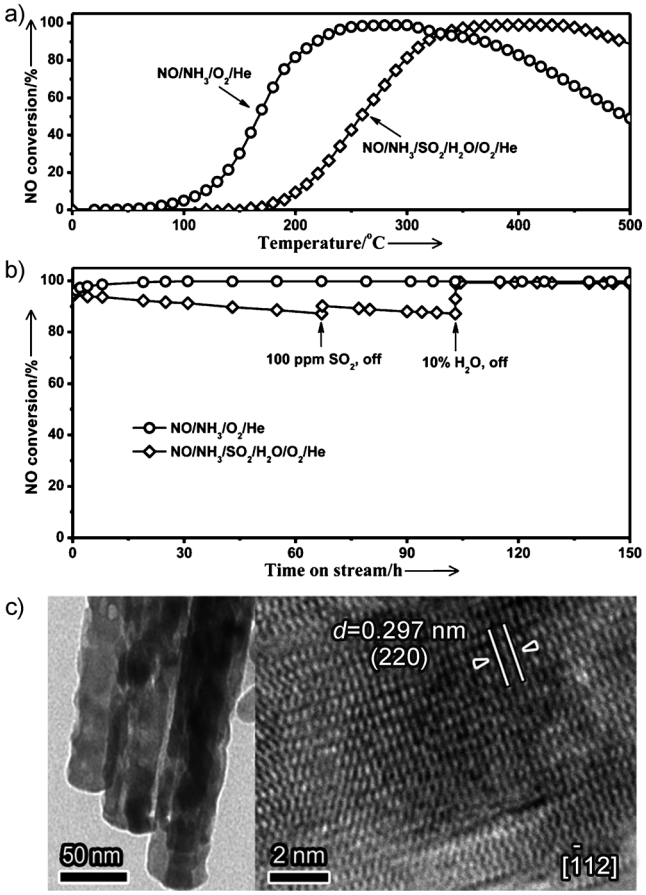

Figure 3. a) NO conversion as a function of temperature with (◇) and without (○) water (10 vol%) and SO_2 ($\delta = 100$ ppm) in the feed gas of $\delta = 1000$ ppm NO/$\delta = 1000$ ppm NH_3/3.0 vol% O_2/He (72000 mL g^{-1} h^{-1}). b) Stability tests at 350 °C for 150 h. c) TEM images of the used catalyst.

achieved at 220 °C. The temperature window for 80% NO conversion ranges from 200 to 400 °C and the selectivity towards N_2 is maintained at about 98% over the whole temperature range (Supporting Information, Figure S6). This salient performance is of utmost importance in NO_x removal at low to medium temperatures. When compared to the industrially used VO_x-based catalysts,[22,23] the less costly and non-toxic Fe_2O_3 nanorods offer fairly compatible or even slightly better efficiency under similar reaction conditions (Supporting Information, Figure S7). As the exhaust usually contains a large amount of H_2O (2–15 vol%) and certain amounts of SO_2 ($\delta = 30$–2000 ppm),[2,24] we further tested the Fe_2O_3 nanorods with a feed stream containing 10 vol% H_2O and $\delta = 100$ ppm SO_2. Because of the adsorption of water on the catalyst surface, the light-off temperature increases to 260 °C and the temperature region for 80% NO conversion shifts to 300–500 °C (Figure 3a). Nevertheless, the pronounced activity and the available temperature window still fulfill the criteria for practical stationary NO_x removal.[2]

The γ-Fe_2O_3 nanorods are very robust both in a transient process with frequent variation in temperature and in a long-term steady operation at a constant temperature. Upon periodically fluctuating the reaction temperature over the range 150–450 °C, the conversion of NO and the selectivity of N_2 are highly reproducible; the temperature region for 80% NO conversion remains at 200–400 °C, and the size and shape of the used catalyst remains unchanged (Supporting Information, Figure S8). When used for a long-term test at 350 °C, a typical temperature in practical applications, NO conversion is maintained at 100% for 150 h (Figure 3b). The addition of H_2O and SO_2 slightly lowers NO conversion to about 90%, but the removal of SO_2 from the reaction gas immediately raises NO conversion to 93%. After cutting off the supply of water, the conversion of NO is rapidly restored to 100% and is kept at this level for the rest of the operation.

This reaction pattern demonstrates that the γ-Fe_2O_3 nanorods are highly sulfur-resistant and the inhibition of water is reversible, thus differing from the traditional iron oxides that are severely and irreversibly deactivated by H_2O and SO_2.[5,6] TEM analyses of the catalyst after the stability test confirm that both the morphology and the exposed facets are almost the same as the fresh one (Figure 3c). Electron energy-loss spectroscopy (EELS) reaffirmed that the oxidation state of iron and the coordination of oxygen in the catalyst keep unchanged before and after the reaction (Table S1 in the Supporting Information), indicating the stable surface coordination environment.

Activation of NH_3 on the catalyst surface is generally viewed as the primary step in SCR of NO, as it is experimentally indentified on VO_x-based catalysts.[25–27] Temperature-programmed desorption (TPD) of NH_3 on the γ-Fe_2O_3 nanorods shows an intense desorption peak of N_2 at 250–430 °C (Figure 4a). As there is no oxygen in the feed gas, the generation of nitrogen originates from the oxidation of adsorbed ammonia by the lattice oxygen of γ-Fe_2O_3. This is also supported by the TPD profile of NH_3/O_2 co-adsorption where the pre-adsorbed molecular oxygen has negligible impact on the desorption pattern of N_2 (Figure 4b). In fact, the Fe_2O_3 nanorods catalyze NH_3 oxidation very efficiently; the conversion of NH_3 and the selectivity towards N_2 are as high as 90% even at 350 °C (Supporting Information, Figure S9), evidencing the facile activation of ammonia. On the other hand, the adsorption of NO is strongly affected by the presence of oxygen molecule. NO is only weakly adsorbed on the Fe_2O_3 nanorods and is easily desorbed below 250 °C (Figure 4c). However, the presence of molecular oxygen greatly promotes the adsorption of NO. The co-adsorption of NO/O_2 yields a strong desorption peak of NO_2 at 372 °C (Figure 4d). This is in accord with a comparative test of NO oxidation on the Fe_2O_3 nanorods where the conversion of NO to NO_2 reaches 26% at about 370 °C (Supporting Information, Figure S9), suggesting that the γ-Fe_2O_3 nanorods enable to catalyze NO oxidation effectively as well.

Catalytically, the outstanding SCR performance of the γ-Fe_2O_3 nanorods is intimately associated with the exposed {110} and {001} planes. Ammonia is well adsorbed on the Lewis acidic Fe^{3+} sites, whereas NO is only weakly adsorbed.[28–30] The inferior performance of the α-Fe_2O_3 nanorods in a comparative test confirms that the exposed {210} and {001} planes are much less active (Supporting Information, Figure S4d,e). This is because these Fe-terminated surfaces in the α phase (space group $R\bar{3}c$ (no. 167)) only provide ferric

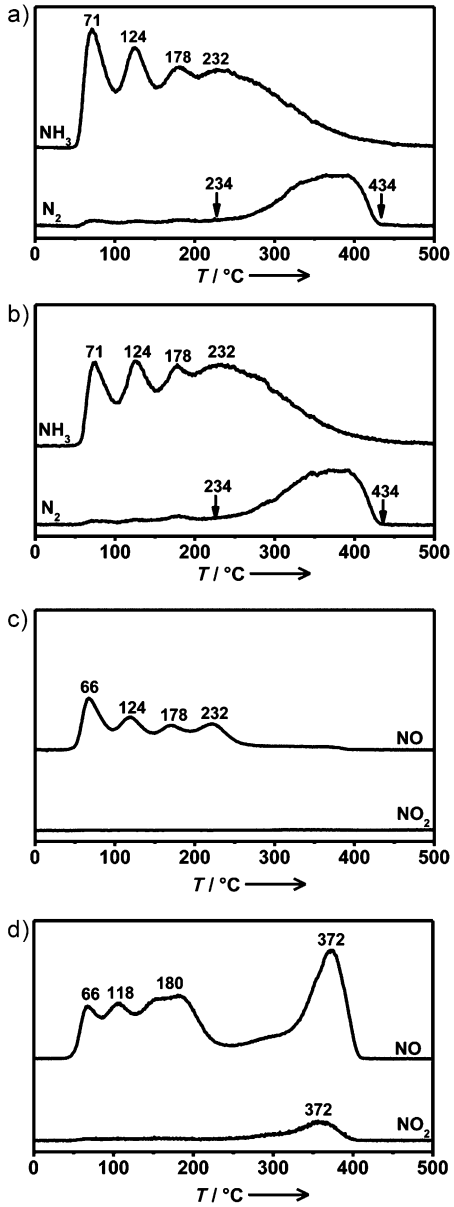

Figure 4. TPD profiles of a) NH_3, b) NH_3/O_2, c) NO, and d) NO/O_2 on the γ-Fe_2O_3 nanorods.

sites for the adsorptions of NO and NH_3 but lack neighboring oxygen anions for their activations. In contrast, the {110} and {001} surfaces on the γ-Fe_2O_3 nanorods contain iron and oxygen ions simultaneously. The ferric site and its neighboring basic oxygen site jointly accomplishes the reactive adsorptions of NO and NH_3, and their subsequent reaction yields nitrogen and water, probably through surface nitrates.[27] The apparent activation energies are 49 and 56 kJ mol^{-1} at 120–160 °C and 340–360 °C, respectively. The turnover frequencies of the Fe^{3+} site are 1.39×10^{-3} s^{-1} at 150 °C and 6.01×10^{-3} s^{-1} at 350 °C (Table S2 in the Supporting Information).

In summary, we have successfully fabricated crystal-phase and morphology controlled Fe_2O_3 nanomaterials. In particular, γ-Fe_2O_3 nanorods that are enclosed by the reactive {110} and {100} facets are highly active and distinctively stable for the SCR of NO with NH_3. This provides a possibility for obtaining highly efficient SCR catalysts using less costly and non-toxic Fe_2O_3 nanomaterials, and potentially offers a new more general strategy to promote the catalytic property of metal oxides by tuning crystal phase and shape at the nanometer level.

Experimental Section

The β-FeOOH nanorods were prepared by an aqueous precipitation method. An aqueous solution containing $FeCl_3\cdot6H_2O$ (5.38 g), NaCl (11.60 g), and PEG (10 mL) in water (190 mL) was gradually heated to 120 °C. A Na_2CO_3 aqueous solution (200 mL, 0.2 M) was then added through a syringe pump at a rate of 5.5 mL min^{-1}. The mixture was then aged at 120 °C for 1 h. The precipitate was washed with water and ethanol, and finally dried at 50 °C for 6 h under vacuum. The γ-Fe_2O_3 nanorods were prepared by heating the β-FeOOH precursor in PEG to reflux. A slurry mixture containing β-FeOOH nanorods (5.0 g) and PEG (500 mL) was gradually heated to 200 °C and heated to reflux for 24 h under a stream of nitrogen. The resulting solid was washed with water and ethanol, followed by drying at 50 °C for 12 h under vacuum.

TEM images were taken on a Philips FEI Tecnai G^2 microscopy operating at 120 kV. HRTEM images were recorded on a FEI Cs-corrected Titan 80–300 microscope operated at 300 kV with a Gatan filter. EELS analyses were performed with an energy dispersion of 0.1 eV. TPD of NO and NH_3 on the γ-Fe_2O_3 nanorods were conducted with a quartz-tube reactor that was connected to a mass spectrometer. 100 mg samples were pre-treated with a 3.0 vol% O_2/He mixture at 400 °C for 0.5 h, followed by NH_3 or NO adsorption at room temperature.

SCR of NO with NH_3 was conducted with a continuous-flow quartz-tube reactor under atmospheric pressure. Before the test, γ-Fe_2O_3 nanorods (100 mg, 40–60 mesh) were treated with a 3.0 vol% O_2/He mixture (60 mL min^{-1}) at 400 °C for 0.5 h. Typically, the feed gas contained $\delta = 1000$ ppm NO, $\delta = 1000$ ppm NH_3, and 3 vol% O_2 balanced with He (120 mL min^{-1}). When necessary, 10.0 vol% H_2O and $\delta = 100$ ppm SO_2 were added to the gas stream. The concentrations of nitrogen oxides and nitrogen in the inlet and outlet streams were continuously detected by a NO/NO_x analyzer and a mass spectrometer.

Received: October 7, 2011
Published online: February 6, 2012

Keywords: iron · heterogeneous catalysis · morphology control · nanoparticles · nitrogen oxides

[1] S. Roy, M. S. Hegde, G. Madras, *Appl. Energy* **2009**, *86*, 2283–2297.
[2] E. Hums, *Catal. Today* **1998**, *42*, 25–35.
[3] R. M. Heck, *Catal. Today* **1999**, *53*, 519–523.
[4] G. Busca, L. Lietti, G. Ramis, F. Berti, *Appl. Catal. B* **1998**, *18*, 1–36.
[5] N. Apostolescu, B. Geiger, K. Hizbullah, M. Jan, S. Kureti, D. Reichert, F. Schott, W. Weisweiler, *Appl. Catal. B* **2006**, *62*, 104–114.
[6] Z. Liu, P. J. Millington, J. E. Bailie, R. R. Rajaram, J. A. Anderson, *Microporous Mesoporous Mater.* **2007**, *104*, 159–170.
[7] F. Liu, H. He, C. Zhang, *Chem. Commun.* **2008**, 2043–2045.
[8] G. H. Yao, K. T. Gui, F. Wang, *Chem. Eng. Technol.* **2010**, *33*, 1093–1098.
[9] L. Machala, J. Tuček, R. Zbořřil, *Chem. Mater.* **2011**, *23*, 3255–3272.

[10] Y. Piao, J. Kim, H. B. Na, D. Kim, J. S. Baek, M. K. Ko, J. H. Lee, M. Shokouhimehr, T. Hyeon, *Nat. Mater.* **2008**, *7*, 242 – 247.
[11] A. Shavel, L. M. Liz-Marzan, *Phys. Chem. Chem. Phys.* **2009**, *11*, 3762 – 3766.
[12] H. G. Cha, S. J. Kim, K. J. Lee, M. H. Jung, Y. S. Kang, *J. Phys. Chem. C* **2011**, *115*, 19129 – 19135.
[13] S. Li, H. Zhang, J. Wu, X. Ma, D. Yang, *Cryst. Growth Des.* **2006**, *6*, 351 – 353.
[14] F. Meng, S. A. Morin, S. Jin, *J. Am. Chem. Soc.* **2011**, *133*, 8408 – 8411.
[15] R. M. Cornell, U. Schwertmann, *The iron oxides*: *structure*, *properties*, *reactions*, *occurrence and uses*, 2nd ed., Wiley-VCH, Weinheim, **2003**, chap. 14, pp. 365 – 405.
[16] N. K. Chaudhari, J. S. Yu, *J. Phys. Chem. C* **2008**, *112*, 19957 – 19962.
[17] S. Sakurai, A. Namai, K. Hashimoto, S. Ohkoshi, *J. Am. Chem. Soc.* **2009**, *131*, 18299 – 18303.
[18] A. Navrotsky, L. Mazeina, J. Majzlan, *Science* **2008**, *319*, 1635 – 1638.
[19] R. J. Armstrong, A. H. Morrish, G. A. Sawatzky, *Phy. Lett.* **1966**, *23*, 414 – 416.
[20] J. E. Jørgensen, L. Mosegaard, L. E. Thomsen, T. R. Jensen, J. C. Hanson, *J. Solid State Chem.* **2007**, *180*, 180 – 185.
[21] V. Petkov, P. D. Cozzoli, R. Buonsanti, R. Cingolani, Y. Ren, *J. Am. Chem. Soc.* **2009**, *131*, 14264 – 14266.
[22] R. Q. Long, R. T. Yang, *J. Catal.* **1999**, *188*, 332 – 339.
[23] H. S. Yang, S. L. Song, H. C. Choi, I. S. Nam, H. J. Chae, US patent 6475944 B1, **2002**.
[24] K. Skalska, J. S. Miller, S. Ledakowicz, *Sci. Total Environ.* **2010**, *408*, 3976 – 3989.
[25] N. Y. Topsøe, *Science* **1994**, *265*, 1217 – 1219.
[26] I. Giakoumelou, C. Fountzoula, C. Kordulis, S. Boghosian, *J. Catal.* **2006**, *239*, 1 – 12.
[27] A. Grossale, I. Nova, E. Tronconi, D. Chatterjee, M. Weibel, *J. Catal.* **2008**, *256*, 312 – 322.
[28] C. H. Rochester, S. A. Topham, *J. Chem. Soc. Faraday Trans.* **1979**, *75*, 1259 – 1267.
[29] Y. Wang, Z. Lei, B. Chen, Q. Guo, N. Liu, *Appl. Surf. Sci.* **2010**, *256*, 4042 – 4047.
[30] K. Otto, M. Shelef, *J. Catal.* **1970**, *18*, 184 – 192.

